

# Mitochondrion as a Novel Site of Dichloroacetate Biotransformation by Glutathione Transferase $\zeta$ 1

Wenjun Li, Margaret O. James, Sarah C. McKenzie, Nigel A. Calcutt, Chen Liu, and Peter W. Stacpoole

Department of Medicinal Chemistry, College of Pharmacy (W.L., M.O.J., S.C.M.) and Departments of Pathology (C.L.) and Medicine and Biochemistry and Molecular Biology (P.W.S.), College of Medicine, University of Florida, Gainesville, Florida; and Department of Pathology, University of California at San Diego, La Jolla, California (N.A.C.)

Received July 26, 2010; accepted September 24, 2010

## ABSTRACT

Dichloroacetate (DCA) is a potential environmental hazard and an investigational drug. Repeated doses of DCA result in reduced drug clearance, probably through inhibition of glutathione transferase  $\zeta$ 1 (GSTZ1), a cytosolic enzyme that converts DCA to glyoxylate. DCA is known to be taken up by mitochondria, where it inhibits pyruvate dehydrogenase kinase, its major pharmacodynamic target. We tested the hypothesis that the mitochondrion was also a site of DCA biotransformation. Immunoreactive GSTZ1 was detected in liver mitochondria from humans and rats, and its identity was confirmed by liquid chromatography/tandem mass spectrometry analysis of the tryptic peptides. Study of rat submitochondrial fractions revealed GSTZ1 to be localized in the mitochondrial matrix. The

specific activity of GSTZ1-catalyzed dechlorination of DCA was 2.5- to 3-fold higher in cytosol than in whole mitochondria and was directly proportional to GSTZ1 protein expression in the two compartments. Rat mitochondrial GSTZ1 had a 2.5-fold higher  $A^{PP}K_m$  for glutathione than cytosolic GSTZ1, whereas the  $A^{PP}K_m$  values for DCA were identical. Rats administered DCA at a dose of 500 mg/kg/day for 8 weeks showed reduced hepatic GSTZ1 activity and expression of ~10% of control levels in both cytosol and mitochondria. We conclude that the mitochondrion is a novel site of DCA biotransformation catalyzed by GSTZ1, an enzyme colocalized in cytosol and mitochondrial matrix.

## Introduction

Dichloroacetate (DCA;  $Cl_2HC-COOH$ ) is a unique xenobiotic that is both a potential environmental hazard and an investigational drug for the treatment of genetic mitochon-

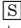
drial diseases (Stacpoole et al., 2008) and certain hyperproliferative conditions, such as pulmonary arterial hypertension and cancer (Archer et al., 2008; Michelakis et al., 2010). DCA is a byproduct of water chlorination, resulting in an exposure level of a few micrograms/kilograms/day to humans through consumption of municipal drinking water (Mughal, 1992). DCA is also formed in vivo as a minor metabolite of certain chlorinated industrial solvents, including trichloroethylene, and pharmaceuticals, such as chloral hydrate and chloramphenicol (Stacpoole et al., 1998). DCA has been considered as a potential health hazard based on extrapolated animal studies that showed multiple organ toxicities and hepatocarcinogenicity in inbred strains of rodents after chronic exposure to doses more than  $10^4$ -fold higher than levels encountered through environmental exposure (Stacpoole et al., 1998). However, similar doses of 10 to 50 mg/kg/day have been used clinically for decades in treating acquired and congenital metabolic disorders and, more recently, cancer (Stacpoole

This work was supported in part by the National Institutes of Health National Institute of Environmental Health Sciences [Grants ES-007355, ES-014617] and the National Institutes of Health National Center for Research Resources [Grant 1UL1-RR-029890] (to P.W.S.).

Part of this work was presented previously: Li W, James MO, McKenzie S, and Stacpoole PW (2010) Mitochondrion is a novel site of biotransformation of dichloroacetate by glutathione transferase zeta, at the *Experimental Biology 2010 Annual Meeting*; 2010 Apr. 24-28; Anaheim, CA. *Experimental Biology*, Bethesda, MD [(2010) *FASEB J.* 24:967.17]; and Li W, James MO, Reid P, and Stacpoole PW (2009) Mitochondria as a site of metabolism of dichloroacetate, at the *Society of Toxicology 48th Annual Meeting*; 2009 March 15-19; Baltimore, MD. *Society of Toxicology*, Reston, VA [(2009) *The Toxicologist* 108:90].

Article, publication date, and citation information can be found at <http://jpet.aspetjournals.org>.

doi:10.1124/jpet.110.173195.

 The online version of this article (available at <http://jpet.aspetjournals.org>) contains supplemental material.

**ABBREVIATIONS:** DCA, dichloroacetate; GSTZ1, glutathione transferase  $\zeta$ 1; hGSTZ1, human GSTZ1; ALDH1A1, aldehyde dehydrogenase 1A1; PDK, pyruvate dehydrogenase kinase; PDH, pyruvate dehydrogenase; IM, inner membrane; IMS, intermembrane space; LC, liquid chromatography; HPLC, high-performance liquid chromatography; MS/MS, tandem mass spectrometry; ESI-QTOF, electrospray ionization hybrid quadrupole time of flight; MWCO, molecular mass cutoff; PAGE, polyacrylamide gel electrophoresis; SD, Sprague-Dawley; OM, outer membrane; CypD, cyclophilin D; CytC, cytochrome C.

et al., 1998, 2008; Michelakis et al., 2010). Adverse effects from chronic DCA administration include mild increases in serum transaminases and mild to severe peripheral neuropathy, both of which are reversible and resolve gradually after discontinuation of the drug (Stacpoole et al., 1998).

DCA is transported across cell membranes by the monocarboxylate transporter system and gains entry into the mitochondrial matrix via the mitochondrial pyruvate transporter (Stacpoole et al., 1998). Within the matrix, DCA inhibits pyruvate dehydrogenase kinase (PDK) that inactivates the pyruvate dehydrogenase (PDH) complex. PDH is a gatekeeper enzyme that regulates the entry of glucose-derived carbon into mitochondria and oxidizes pyruvate to acetyl CoA. By inhibiting PDK, DCA activates PDH, which increases the provision of acetyl CoA to the Krebs cycle and, in turn, stimulates oxidative phosphorylation. By shifting the metabolism of glucose from glycolysis and lactate formation to mitochondrial oxidative phosphorylation, DCA reduces lactate concentrations and reverses the Warburg effect in pulmonary artery smooth muscle cells and cancer cells (Archer et al., 2008; Stacpoole et al., 2008; Michelakis et al., 2010). For these reasons, the mitochondrion is considered to be the primary cellular site of DCA action.

DCA is eliminated mainly through glutathione transferase  $\zeta 1$  (GSTZ1)-catalyzed dechlorination to glyoxylate, an intermediate that is further metabolized primarily by mitochondrial enzymes before excretion (Supplemental Fig.1). GSTZ1 is the only GST known to metabolize DCA. A trace amount of DCA can also be reductively dechlorinated to monochloroacetate in the blood (Shroads et al., 2008). In vivo exposure to DCA causes a dose- and duration-dependent reduction in hepatic GSTZ1 expression and activity (Cornett et al., 1999; Ammini et al., 2003). Accordingly, DCA exhibits reduced plasma clearance and prolonged elimination half-life after repeated exposure (Stacpoole et al., 1998).

GSTZ1 is a member of the cytosolic GST superfamily. Like other GSTs, GSTZ1 is present in the cytosol and is most abundantly expressed in the liver (Lantum et al., 2002). Over the past decade, increasing numbers of drug-metabolizing enzymes have been shown to exist in multiple subcellular compartments. These include several cytosolic GSTs (GSTA1, GSTA2, GSTA4, GSTP1, and GSTM1) that were found to be localized in the hepatic mitochondria (Raza et al., 2002; Gallagher et al., 2006). Because DCA is known to be taken up by the mitochondria, we tested the postulate that this organelle is also a site of DCA biotransformation by examining the expression and activity of GSTZ1 in liver mitochondria from humans and rats.

## Materials and Methods

**Subcellular Fractionation of Human and Rat Livers.** Adult female Sprague-Dawley (SD) rats were treated by gavage with tap water vehicle ( $n = 9$ , control group) or 500 mg/kg/day DCA ( $n = 11$ , DCA-treated group) for 8 weeks. Neuropathy was confirmed by measuring sciatic motor nerve conduction velocity and paw thermal response latency exactly as described elsewhere followed by sacrifice by decapitation (Calcutt et al., 2009). Studies were performed after approval by the local Institutional Animal Care and Use Committee. De-identified normal human liver samples (1–2 g) were collected during surgery under a protocol approved by the Institutional Review Board of Shands Hospital at the University of Florida (Gaines-

ville, FL) for use in these studies. Livers were quickly removed, snap-frozen in liquid nitrogen, and stored at  $-80^{\circ}\text{C}$  until use.

Frozen liver was thawed and rinsed in ice-cold homogenizing buffer (0.25 M sucrose, 0.02 M HEPES-NaOH, pH 7.4 and 0.1 mM phenylmethanesulfonyl fluoride). Rinsed livers were minced and homogenized in five volumes of homogenizing buffer with a motor-driven Teflon pestle for four complete strokes. After sedimenting the nuclei and cell debris at 600g, mitochondria were pelleted by centrifuging the supernatant at 13,000g for 20 min. The 13,000g supernatant was further subjected to differential centrifugation to isolate cytosol and washed microsomes (James et al., 1976). The mitochondrial pellet was resuspended and washed twice before being taken up in the resuspension buffer (0.25 M sucrose, 0.01 M HEPES-NaOH, pH 7.4, 0.1 mM dithiothreitol, 0.1 mM EDTA, 0.1 mM phenylmethanesulfonyl fluoride, and 5% glycerol) in a volume equal to the liver weight. The washed mitochondria and cytosol were stored in aliquots at  $-80^{\circ}\text{C}$  until use. All procedures were performed at  $4^{\circ}\text{C}$  or on ice. Cytosol and mitochondria were dialyzed with 10-kDa MWCO Slide-A-Lyzer Dialysis Cassettes (Thermo Fisher Scientific, Waltham, MA) against 1.15% KCl and 0.05 M potassium phosphate buffer, pH 7.4 before use for assays. Protein concentrations were determined by the Bradford method (Bio-Rad Laboratories, Hercules, CA) using bovine serum albumin (Sigma-Aldrich, St. Louis, MO) as protein standard.

**Subfractionation of Liver Mitochondria.** Three 9-week old male SD rats were killed by decapitation, and their livers were quickly isolated and rinsed in ice-cold homogenizing buffer to remove blood. The washed mitochondria were immediately isolated by the procedures described above and subfractionated as follows. The suspension of washed mitochondria was diluted with swelling buffer (0.01 M Tris-HCl, pH 7.4) to a final sucrose concentration of  $\sim 0.05$  M and gently mixed with a magnetic stirrer at  $4^{\circ}\text{C}$  for 15 min. Shrinking buffer (2 M sucrose, 100 mM Tris-HCl, pH 7.4) was then added into the swelled mitochondria to a final sucrose concentration of  $\sim 0.3$  M. After another 15-min stirring, the swollen-and-shrunk (shocked) mitochondria were centrifuged at 20,000g for 20 min. The supernatant yielded the intermembrane space (IMS) proteins. The pellet of shocked mitochondria was washed once, resuspended in homogenizing buffer, and stored at  $-80^{\circ}\text{C}$ . After three cycles of freezing and thawing, the shocked mitochondria were further subjected to three strokes of homogenization by Dounce homogenizer and five cycles of 5-s sonication at 25-s intervals. The shocked mitochondria were then centrifuged at 125,000g for 60 min to sediment the total mitochondrial membrane with the mitochondrial matrix remaining in the supernatant. The pellet containing the total mitochondrial membrane was resuspended in resuspension buffer. The IMS protein and matrix protein were concentrated by filtering through Amicon Ultra 15-ml filters of 10-kDa MWCO (Millipore Corporation, Billerica, MA).

**Electrophoresis and Western Blots.** Known amounts of denatured protein were separated on 4 to 15% SDS-PAGE (Tris-HCl Gel; Bio-Rad Laboratories) and subsequently electrotransferred onto polyvinylidene fluoride membrane (Millipore Corporation). Purified recombinant human GSTZ1C-1C was obtained as described previously (Guo et al., 2006) and used as positive control. After blocking, the membrane was incubated overnight at  $4^{\circ}\text{C}$  with primary antibodies, 1:2000 rabbit polyclonal anti-hGSTZ1C-1C (Cocalico Biologicals, Inc., Reamstown, PA), 10.2  $\mu\text{g}/\text{ml}$  mouse monoclonal Mito-Profile Membrane Integrity WB Antibody Cocktail (MitoSciences, Eugene, OR), or 1:2000 rabbit monoclonal anti-aldehyde dehydrogenase 1A1 (ALDH1A1) (Abcam Inc., Cambridge, MA). The membrane was then washed and incubated with corresponding secondary antibodies, horseradish peroxidase-conjugated donkey anti-rabbit IgG, 1:2000 or sheep anti-mouse IgG F(ab')<sub>2</sub> 1:5000 (GE Healthcare, Chalfont St. Giles, Buckinghamshire, UK). Protein signal was developed by Pierce ECL substrate (Thermo Fisher Scientific) on Amersham Hyperfilm ECL (GE Healthcare) according to the manufacturers' instructions. For quantitative analysis, the resulting hyperfilm was digitized by scanning, and the density of bands was quan-

titated by ImageJ software (version 1.41o; National Institutes of Health, Bethesda, MD).

**GSTZ1 Activity.** The specific activity of GSTZ1 was measured by using [ $^{14}\text{C}$ ]-DCA (American Radiolabeled Chemicals, St. Louis, MO) as substrate, and assay products were measured by an HPLC method coupled with radiochemical detection (James et al., 1997). Assay conditions were optimized to achieve linearity of product formation with incubation time and protein concentration; substrate consumption did not exceed 15%. To determine the maximum reaction rate, assay tubes containing 0.2 mM  $^{14}\text{C}$ -DCA in 0.1 M HEPES-NaOH, pH 7.6 were incubated with either cytosolic protein and 2 mM GSH or mitochondrial protein and 5 mM GSH in a volume of 0.1 ml. After a 2-min preincubation at 37°C, the reaction was started by adding  $^{14}\text{C}$ -DCA. Tubes were incubated at 37°C with gentle shaking for 15 min, after which the reaction was stopped by adding 0.1 ml of ice-cold methanol. For the submitochondrial experiment, enzyme-specific activity was measured with 0.2 mM DCA and 2 mM GSH over 30-min incubation for all fractions. For kinetic studies cytosol and mitochondria were incubated with varying concentrations of GSH and DCA over adjusted incubation times, as specified in *Results*. The kinetic parameters ( $V_{\text{max}}$  and  $K_m$ ) were derived with the software Prism version 4.03 (GraphPad Software, Inc., San Diego, CA) by fitting the data to the Michaelis-Menten equation,  $v = V_{\text{max}}[S]/(K_m + [S])$ . Goodness of fit to the Michaelis-Menten equation was determined by the software.

**Immunoprecipitation of Mitochondrial GSTZ1.** Soluble mitochondrial protein of human liver and mitochondrial matrix protein of rat liver were used for immunoprecipitation of GSTZ1. To obtain the soluble mitochondrial protein of human liver, the washed human liver mitochondria were frozen and thawed three times, and then diluted to approximately 2 mg/ml in homogenizing buffer. After sonication and homogenization, the disrupted mitochondria were centrifuged at 125,000g for 60 min to pellet the total mitochondrial membrane. The soluble mitochondrial protein was collected from the supernatant and further concentrated by using Amicon Ultra 15-ml filters of 10-kDa MWCO.

Immunoprecipitation of mitochondrial GSTZ1 was carried out with the Pierce Direct IP kit (Thermo Fisher Scientific) following the provider's instructions. For each column, 10  $\mu\text{g}$  of human GSTZ1C-1C antibody was coupled to 30  $\mu\text{l}$  of 50% slurry of AminoLink Plus coupling resin. Mitochondrial protein (500  $\mu\text{g}$ ) was incubated with the antibody-coupled resin overnight at 4°C. After centrifuging the mixture to remove unbound proteins, the resin was washed with immunoprecipitation lysis/wash buffer supplied by the kit. The antigen was then eluted with the primary amine-containing, pH 2.8 elution buffer supplied by the kit. Eluants were neutralized with 1 M Tris-HCl, pH 9.5 in a 10:1 ratio. For each species, eluants from three columns were pooled and concentrated through Amicon Ultra 0.5-ml filters of 10-kDa MWCO (Millipore Corporation). The concentrated eluants were denatured and separated on 4 to 15% SDS-PAGE. Protein bands from the rat or human samples that migrated to the same position as the positive control, purified human GSTZ1C, were excised and digested with trypsin (Sheffield et al., 2006) for LC-MS/MS protein identification.

**LC-MS/MS.** The trypsin-digested samples were injected onto a capillary trap (LC Packings PepMap; Dionex Corporation, Sunny-

vale, CA) and washed for 5 min with a flow rate of 10  $\mu\text{l}/\text{min}$  of 0.1% (v/v) acetic acid. The samples were loaded onto a LC Packings C18 PepMap HPLC column (Dionex Corporation). The elution gradient of the HPLC column started at 97% solvent A (0.1% v/v acetic acid, 3% v/v acetonitrile, and 96.9% v/v water), 3% solvent B (0.1% v/v acetic acid, 96.9% v/v acetonitrile, and 3% v/v water) and finished at 40% solvent A, 60% solvent B for 60 min. LC-MS/MS analysis was carried out on a hybrid quadrupole-TOF mass spectrometer (QSTAR; Applied Biosystems, Framingham, MA). The focusing potential and ion spray voltage were set to 275 and 2600 V, respectively. The information-dependent acquisition mode of operation was used in which a survey scan from  $m/z$  400 to 1200 was acquired followed by collision-induced dissociation of the three most intense ions. Survey and MS/MS spectra for each information-dependent acquisition cycle were accumulated for 1 and 3 s, respectively.

**Protein Search Algorithm.** Tandem mass spectra were extracted by ABI Analyst version 1.1 (AB SCIEX, Toronto, Canada). All MS/MS samples were analyzed using Mascot (version 2.2.2; Matrix Science, London, UK). Mascot was set up to search the International Protein Index database with trypsin as the digestive enzyme. Mascot was searched with a fragment ion mass tolerance of 0.30 Da and a parent ion tolerance of 0.30 Da. Iodoacetamide derivative of Cys, deamidation of Asn and Gln, and oxidation of Met were specified in Mascot as variable modifications. Scaffold 2 (version Scaffold-02.03.01; Proteome Software Inc., Portland, OR) was used to validate MS/MS-based peptide and protein identifications. Peptide identifications were accepted if they could be established at more than 95.0% probability, as specified by the Peptide Prophet algorithm (Keller et al., 2002). Protein identifications were accepted if they could be established at more than 99.0% probability and contained at least two identified unique peptides. Protein probabilities were assigned by the Protein Prophet algorithm (Nesvizhskii et al., 2003).

## Results

**DCA Toxicity.** DCA treatment for 8 weeks induced mild weight loss (control =  $282 \pm 5$  versus DCA =  $259 \pm 3$  g; mean  $\pm$  S.E.M.,  $p < 0.001$  by unpaired  $t$  test) and peripheral neuropathy, as illustrated by slowing of motor nerve conduction velocity (control =  $50.3 \pm 1.9$  versus DCA =  $42.5 \pm 1.1$  m/s;  $p < 0.01$ ) and paw thermal hypoalgesia (control =  $10.35 \pm 0.62$  versus DCA =  $13.34 \pm 0.72$  s;  $p < 0.001$ ), as has been reported for rats treated with a similar dose of DCA (Calcutt et al., 2009).

**Expression and Activity of GSTZ1 in Hepatic Mitochondria.** In liver mitochondria of both human and rat, our hGSTZ1 antibody cross-reacted with a protein that migrated similarly to the purified hGSTZ1 and the cytosolic GSTZ1 at  $\sim 24$  kDa (Fig. 1). GSTZ1 immunoreactivity was more intense in cytosol than in mitochondria for a given amount of protein, indicating a more abundant expression of GSTZ1 in cytosol. To assure that the detection of mitochondrial immunoreactive GSTZ1 was not caused by cytosolic contamination, mi-

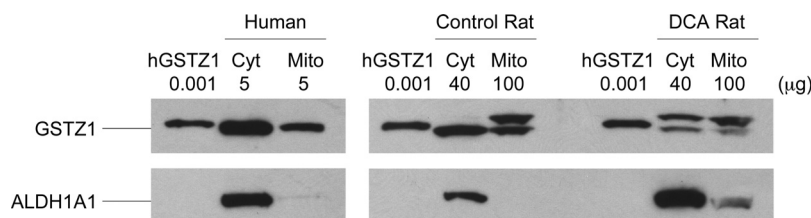


**Fig. 1.** Representative Western blot of immunoreactive GSTZ1 in the liver cytosol (Cyt) and mitochondria (Mito) of human, control rat, and DCA rat. Shown are cytosol and mitochondria of one individual from each group. The DCA rat was exposed to 500 mg/kg/day DCA for 8 weeks before preparation of subcellular fractions. A rabbit polyclonal antibody against human GSTZ1C-1C was used. ALDH1A1 was used as a cytosolic marker to monitor mitochondria purity. hGSTZ1, purified recombinant human GSTZ1C-1C. Protein loading of each sample is indicated.

TABLE 1

Expression and activity of GSTZ1 in the liver cytosol and mitochondria of human, control rat, and DCA rat  
Data are shown as mean  $\pm$  S.D.

	GSTZ1 Expression per Gram Liver <sup>a</sup>		GSTZ1 Expression per Milligram Protein <sup>a</sup>		GSTZ1 Activity <sup>b</sup>	
	Cytosol <sup>c</sup>	Mitochondria <sup>c</sup>	Cytosol	Mitochondria	Cytosol	Mitochondria
Human ( <i>n</i> = 4)	40.1 $\pm$ 11.8	6.78 $\pm$ 1.11	0.54 $\pm$ 0.10	0.23 $\pm$ 0.04	0.49 $\pm$ 0.08	0.20 $\pm$ 0.07
Control rat ( <i>n</i> = 4)	0.92 $\pm$ 0.06	0.14 $\pm$ 0.01	0.94 $\pm$ 0.07	0.24 $\pm$ 0.02	1.47 $\pm$ 0.09	0.48 $\pm$ 0.02
DCA rat ( <i>n</i> = 4)	0.11 $\pm$ 0.03	0.012 $\pm$ 0.003	0.10 $\pm$ 0.02	0.021 $\pm$ 0.006	0.11 $\pm$ 0.06 <sup>d</sup>	N.D.

N.D., not detectable.

<sup>a</sup> GSTZ1 expression was analyzed by using 5  $\mu$ g of human cytosol, 5  $\mu$ g of mitochondria, 40  $\mu$ g of rat cytosol, and 100  $\mu$ g of rat mitochondria on Western blots probed with hGSTZ1 polyclonal antibody. Band intensity was quantitated by ImageJ software. For human samples, the amounts of GSTZ1 were quantitated by comparing the immuno-intensity to a standard curve constructed with pure hGSTZ1. Data are shown as  $\mu$ g hGSTZ1/g liver or  $\mu$ g hGSTZ1/mg protein. For rat samples, individual GSTZ1 expression was normalized as a fraction of one control cytosol that had highest level of GSTZ1 expression. Data are shown as relative GSTZ1 expression/g liver or relative GSTZ1 expression/mg protein.

<sup>b</sup> Samples were dialyzed in 1.15% KCl, 0.05 M potassium phosphate buffer, pH 7.4 before being assayed with 0.2 mM <sup>14</sup>C-DCA as substrate.

<sup>c</sup> Cytosolic yield was calculated based on the total cytosolic protein recovered experimentally. Mitochondrial yield was standardized to 30 mg of mitochondrial protein per gram liver to correct for loss of mitochondria during differential centrifugation (Fleischer et al., 1979).

<sup>d</sup> Of the cytosol of four DCA rats, only two showed detectable activities. The limit of detection was 0.067 nmol/min/mg.

tochondrial purity was established by demonstrating minimal detection of the cytosolic marker ALDH1A1. Cytosolic expression of GSTZ1 was 2.4- and 3.9-fold higher than mitochondrial in human and rat livers, respectively, on a per-milligram of protein basis (Table 1). This is consistent with the 2.5- to 3-fold higher activity of GSTZ1 in cytosol than in mitochondria, as determined using <sup>14</sup>C-DCA as substrate. Approximately 86% [human: 40.1/(40.1 + 6.78); rat: 0.92/(0.92 + 0.14)] of cellular GSTZ1 was located in cytosol and 14% was located in mitochondria, based on the higher yield of protein from cytosol than mitochondria and assuming that 30 mg of mitochondria were present per gram of liver (Fleischer et al., 1979).

GSTZ1 is known to be inactivated by DCA after repeated exposure (Cornett et al., 1999). This was confirmed by the marked reduction in both the expression and activity of cytosolic GSTZ1 in rats treated with 500 mg/kg/day DCA for 8 weeks (Fig. 1 and Table 1). The expression of mitochondrial GSTZ1 in these rats was also reduced to  $\sim$ 10% of control levels, and the specific activity was reduced to below the detection limit (Table 1). Coincidentally, we observed a strong induction of cytosolic marker ALDH1A1 in the DCA-treated rats compared with control rats.

Our GSTZ1 antibody cross-reacted with an unknown protein in rat mitochondria that appeared 1 to 2 kDa larger than GSTZ1 on SDS-PAGE (Fig. 1). The cytosolic expression of this cross-reacting protein changed from not detectable in fresh control livers to barely detectable in frozen control livers to readily detectable in frozen DCA-treated livers (Supplemental Figure 2). This pattern of expression is similar to those of mitochondrial matrix protein cyclophilin D (CypD) and intermembrane space protein cytochrome C (CytC). Preliminary investigation of this protein by immunoprecipitation and LC-MS/MS protein identification suggested that it was a mitochondrial matrix protein with less than 3% sequence identity to hGSTZ1 (National Center for Biotechnology Information Blastp). This result was further supported by its submitochondrial localization in the matrix (see below; Fig. 2A).

**Mitochondrial GSTZ1 Is Localized in the Matrix.** The mitochondrion has a double-membrane structure that divides the organelle into four compartments: the outer membrane (OM), the IMS, the inner membrane (IM), and the matrix. To investigate whether DCA biotransformation oc-

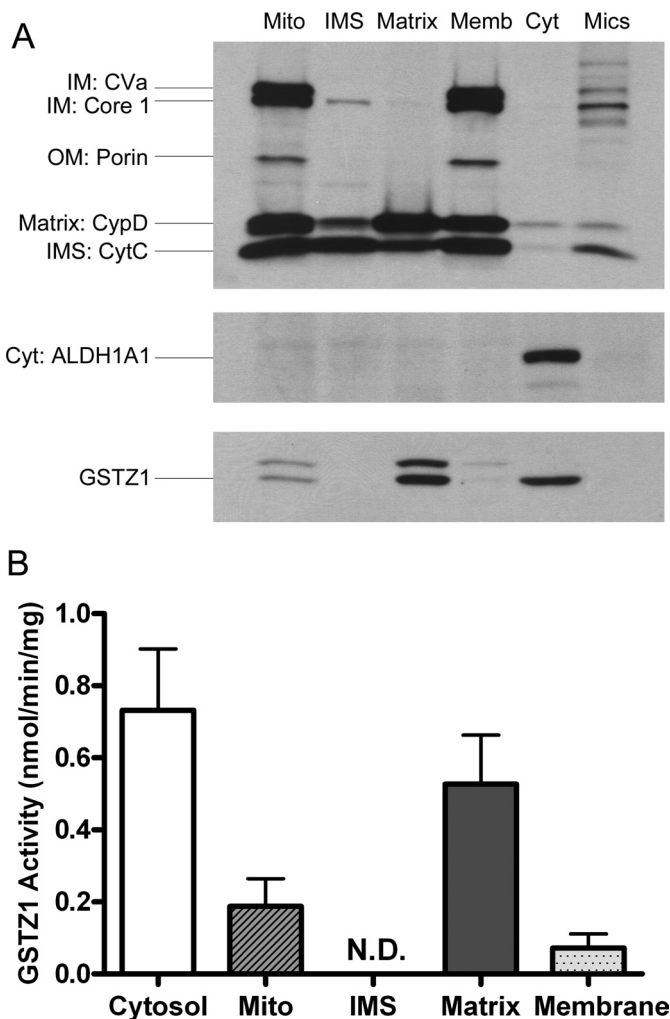


**Fig. 2.** Enrichment of GSTZ1 expression (A) and activity (B) in the matrix of rat liver mitochondria. A, representative Western blot of GSTZ1 expression in the subcellular and submitochondrial fractions of rat liver. Each fraction was loaded with equal amounts of protein, and the fraction identities were confirmed by the predominant expression of respective marker proteins: ALDH1A1 for cytosol (Cyt), complex V subunit a (CVa), and complex III subunit core 1 for mitochondrial IM, porin for mitochondrial OM, CypD for mitochondrial matrix, and CytC for mitochondrial IMS. Mito., washed mitochondria; Memb., mitochondrial membranes; Mics., microsomes. B, GSTZ1 activity in the cytosol and submitochondrial fractions of rat livers measured with 0.2 mM <sup>14</sup>C-DCA as substrate is shown. Data are shown as mean  $\pm$  S.D. of three rats. N.D., not detectable.

curs in the same mitochondrial compartment as its pharmacodynamic action, we examined GSTZ1 expression and activity in the washed mitochondria and three submitochondrial fractions: IMS, the matrix, and the membranes (including OM and IM) (Fig. 2). GSTZ1 expression and catalytic activity were greatest in the matrix, being nearly three times higher than in washed mitochondria. Low levels of GSTZ1 expression and activity were found in the membrane fraction, which might be caused by incomplete release of matrix protein from the shocked mitochondria during fractionation. However, neither expression nor activity was detectable in the IMS. We also confirmed that GSTZ1 exists in cytosol, but not in microsomes. Similar levels of GSTZ1 expression were detected in cytosol and mitochondrial matrix. However, the cytosolic marker ALDH1A1 was detected only in cytosol but not in mitochondrial matrix. This also indicated that the presence of GSTZ1 in mitochondria was not caused by cytosolic contamination.

#### LC-MS/MS Identification of the Mitochondrial GSTZ1.

The identity of the mitochondrial GSTZ1 was verified by immunoprecipitating the antibody-reactive proteins from human and rat liver mitochondria and analyzing the tryptic peptide sequences by LC-ESI-QTOF. We used the matrix protein of rat mitochondria and the soluble protein of human mitochondria for immunoprecipitation. The immunoprecipitated GSTZ1 of

human liver mitochondria was identified with three unique peptides in four unique spectra, covering 12% (27/216) of the hGSTZ1 protein sequence (Fig. 3 and Table 2). Although the coverage was relatively low, a clear ladder of fragmentation was shown in the peptide,  $^{41}\text{DGGQQFSK}^{48}$  (Fig. 4), which increased our confidence of the protein identification. Of the immunoprecipitated rat GSTZ1, two unique peptides covering 13% (28/216) of the rat GSTZ1 protein sequence were identified (Fig. 3 and Table 2).

#### Kinetic Study of Cytosolic and Mitochondrial GSTZ1.

Rat mitochondrial GSTZ1 had a 2.5-fold higher  $^{APP}K_m$  for GSH than the cytosolic GSTZ1, whereas the  $^{APP}K_m$  values for DCA were identical (Table 3). With either GSH or DCA as the variable substrate, the  $^{APP}V_{max}$  values of cytosolic GSTZ1 were three times those of mitochondrial GSTZ1, in good accordance with the 3.9-fold higher expression of cytosolic GSTZ1 per milligram of protein (Table 1). Lineweaver-Burk plots of cytosolic GSTZ1 and mitochondrial GSTZ1 with GSH and DCA as substrates are shown for one representative rat in Fig. 5.

## Discussion

The mitochondrion is the primary site of DCA's pharmacodynamic action. However, its role in DCA biotransformation has been largely overshadowed by the prominence of

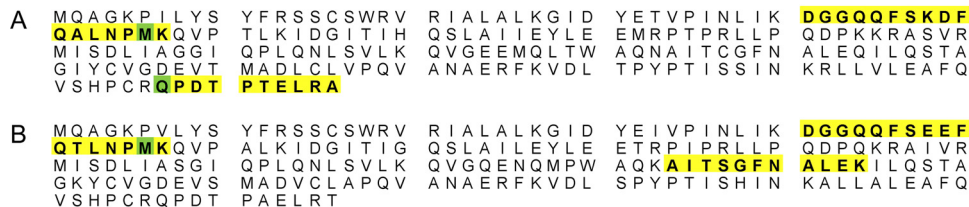


**Fig. 3.** LC-ESI-QTOF analysis of the tryptic peptides of human (A) and rat (B) mitochondrial GSTZ1. A, amino acid sequence of human GSTZ1 (National Center for Biotechnology Information accession no. NP\_665877). B, amino acid sequence of rat GSTZ1 (National Center for Biotechnology Information accession no. NP\_001102915). Peptide fragments identified by MS are highlighted in yellow, and modified amino acids are highlighted in green.

TABLE 2

Characteristics of unique spectra of tryptic peptides of human and rat mitochondrial GSTZ1 identified by ESI-QTOF with 95% probability (calculated by using Scaffold 2 software)

Underlined amino acids were identified by MS with modifications.

Peptide Sequence	Modifications Identified by Spectrum	Mascot Ion Score	Observed $m/z$	Actual Peptide Mass	Spectrum Charge	Actual Minus Calculated Peptide Mass
<b>Human</b>						
41 <u>DGGQQFSK</u> 48		56.8	433.64	865.27	2	-0.12
49 <u>DFQALNPMK</u> 57	Oxidation (+16)	43.2	540.12	1078.23	2	-0.28
207 <u>QPDTPTELRA</u> 216	Pyro-Glu <sup>a</sup> (-17)	49.0	555.71	1109.39	2	-0.14
207 <u>QPDTPTELRA</u> 216		42.5	564.24	1126.46	2	-0.10
<b>Rat</b>						
41 <u>GGQQFSEEFQTLNPMK</u> 57	Oxidation (+16)	37.9	657.87	1970.60	3	-0.27
134 <u>AITSGFNALEK</u> 144		57.1	575.73	1149.44	2	-0.16

<sup>a</sup> Pyroglutamate (Pyro-Glu) formed from cyclization of N-terminal glutamine.

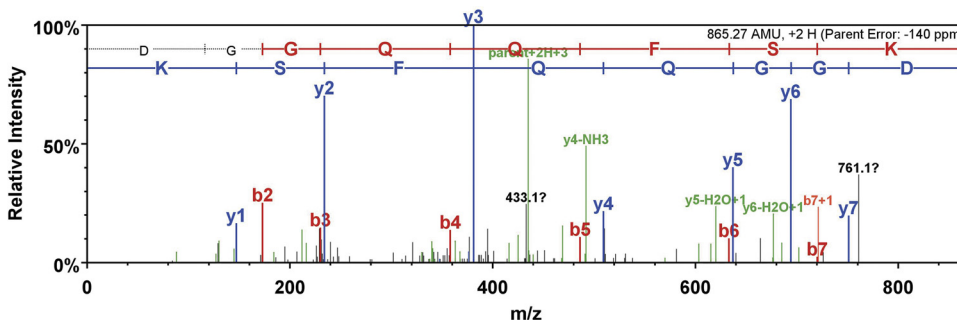


**Fig. 4.** MS/MS fragmentation of the peptide  $^{41}\text{DGGQQFSK}^{48}$  of human mitochondrial GSTZ1.

TABLE 3

Michaelis-Menten parameters of the glutathione-dependent biotransformation of DCA in the dialyzed cytosol and mitochondria of rat livers. Rat liver mitochondria and cytosol were dialyzed at 4°C overnight with three changes of 1.15% KCl, 0.05 M potassium phosphate buffer pH 7.4. Data are shown as mean  $\pm$  S.D. of three rats.

	GSH <sup>a</sup>		DCA <sup>b</sup>	
	<sup>App</sup> K <sub>m</sub>	<sup>App</sup> V <sub>max</sub>	<sup>App</sup> K <sub>m</sub>	<sup>App</sup> V <sub>max</sub>
	mM	nmol/min/mg	mM	nmol/min/mg
Rat mitochondria	0.50 $\pm$ 0.12	0.56 $\pm$ 0.12	0.033 $\pm$ 0.002	0.57 $\pm$ 0.01
Rat cytosol	0.19 $\pm$ 0.04**	1.67 $\pm$ 0.14	0.033 $\pm$ 0.005	1.66 $\pm$ 0.15

<sup>a</sup> With 0.2 mM DCA as substrate, cytosol was incubated with 0.05 to 2.5 mM GSH for 10 min, and mitochondria were incubated with 0.1 to 7.5 mM GSH for 15 min.

<sup>b</sup> With DCA concentration range of 0.005 to 0.2 mM, cytosol was incubated with 2 mM GSH for 5 min, and mitochondria were incubated with 5 mM GSH for 10 min.

\*\**P* < 0.01 compared with <sup>App</sup>K<sub>m</sub> of mitochondria for GSH, analyzed by one-tailed *t* test.

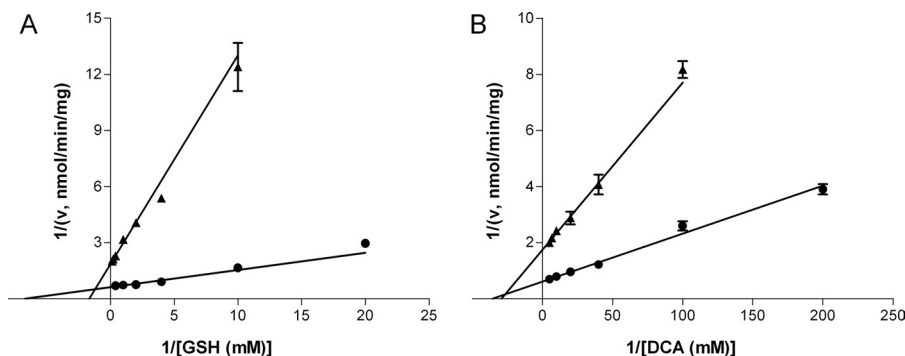


**Fig. 5.** Lineweaver-Burk plots of the rate of DCA biotransformation (*v*) versus the concentrations of cosubstrate GSH (A) and substrate DCA (B) in the liver cytosol (●) and mitochondria (▲). The lines were constructed by using *K<sub>m</sub>* and *V<sub>max</sub>* values obtained from Michaelis-Menten equation, and intercept  $1/V_{max}$  on the y-axis and  $-1/K_m$  on the x-axis. Data are shown as mean  $\pm$  S.E.M. of assay duplicates from one representative rat.

cytosol and endoplasmic reticulum in drug metabolism. In this study we demonstrate the mitochondrion to be a second site of DCA biotransformation in a reaction catalyzed by GSTZ1, an enzyme colocalized in the mitochondrial matrix and cytosol. Furthermore, GSTZ1 expression and activity in the liver mitochondria are susceptible to DCA inactivation, as occurs with the cytosolic form of GSTZ1. We also verified partial sequences of mitochondrial GSTZ1 by LC-MS/MS and compared the kinetics between cytosolic and mitochondrial GSTZ1 by using DCA and GSH as substrates.

The level of GSTZ1 expression is similar in cytosol and mitochondrial matrix, whereas it is approximately 70% less in intact mitochondria on a per-milligram of protein basis. Although a low level of cytosolic contamination was to be expected in the liver mitochondria isolated by differential centrifugation, we confirmed the authenticity of mitochondrial GSTZ1 by demonstrating minimal codetection of cytosolic marker ALDH1A1. Moreover, we would expect to detect any cytosol-originated GSTZ1 in the IMS fraction, which was obtained from the first supernatant of osmotically shocked mitochondria. In fact, GSTZ1 was detected in the mitochondrial matrix at an intensity similar to that in cytosol, but without detectable ALDH1A1 (Fig. 2). This evidence firmly established the mitochondrial origin of GSTZ1. In light of this finding, we searched the literature for GSTZ1 identification from studies of mitochondrial proteome. Indeed, GSTZ1 was identified in the mitochondrial proteome of mouse liver, heart, and kidney (Mootha et al., 2003). Consistent with our finding, GSTZ1 was shown in the proteome of mitochondrial matrix but not the intermembrane space of rat liver (Forner et al., 2006).

Proteins targeted to the mitochondrial matrix usually possess a 15- to 40-amino acid presequence at the N terminal that forms an amphipathic helix to interact with mitochondrial transport machinery during translocation, and the presequence is often cleaved off on import. A few matrix target-

ing proteins with noncleaved presequences or C-terminal presequences have also been identified (Pfanner and Geissler, 2001). All GSTs (GSTA1, GSTA2, GSTA4, GSTP1, and GSTM1) that are currently known to colocalize in cytosol and mitochondrial matrix have similar molecular sizes and identical N terminals in both compartments (Raza et al., 2002; Gallagher et al., 2006). Mitochondrial import studies of GSTA4 and GSTM1 suggest noncleaved internal targeting sequences at the C and N terminals, respectively, of the mature GST proteins (Robin et al., 2003; Goto et al., 2009). Furthermore, protein kinase A- and protein kinase C-catalyzed phosphorylation has been shown to facilitate GSTA4 translocation to the matrix (Robin et al., 2003). The present study of cytosolic and mitochondrial GSTZ1 also suggests their similar molecular weights, as shown by the indistinguishable rates of migration on SDS-PAGE. To obtain more insight into protein structure, we attempted direct N-terminal sequencing for human mitochondrial GSTZ1 immobilized on polyvinylidene fluoride membrane. However, the study failed because of the blocked N terminus, which was also observed for rat cytosolic GSTZ1 (Tong et al., 1998b). On the other hand, one tryptic peptide of human mitochondrial GSTZ1 identified by LC-MS/MS shared the same identity as the C-terminal amino acids of cytosolic GSTZ1, suggesting that the C terminus of GSTZ1 remained intact after mitochondrial import. Therefore, if a mitochondrial targeting sequence of GSTZ1 exists, it may reside within the mature protein and not undergo proteolysis on import.

GSTZ1 of both cytosol and mitochondria catalyzes GSH-dependent dechlorination of DCA, exhibiting the same <sup>App</sup>K<sub>m</sub> values (0.033 mM) for DCA, but a 2.5-fold difference in <sup>App</sup>K<sub>m</sub> values for GSH (0.50 mM mitochondria versus 0.19 mM cytosol). Of cytosolic GSTZ1, the <sup>App</sup>K<sub>m</sub> for GSH obtained currently using female SD rats is 2.5-fold higher than we reported previously using male SD rats (James et al., 1997) and is 3.2-fold higher than the study by Tong et al., (1998a)

using male Fisher 344 rats, in which a 2-fold higher  $^{APP}K_m$  for DCA was also found. The higher  $^{APP}K_m$  for GSH observed with mitochondrial GSTZ1 suggests that it has a weakened access or binding to GSH compared with its cytosolic counterpart. Inspection of the crystal structure of hGSTZ1A-1A with GSH revealed that GSH bound in a deep crevice with close interaction with the active site residues Ser14-Ser15-Cys16 near the N terminus (Polekhina et al., 2001). Cys16 was found to be particularly important in maintaining proper binding and orientation with GSH. Mutation of Cys16 to Ala caused dramatic increases in  $K_m$  values for GSH with various substrates (Board et al., 2003; Ricci et al., 2004). As demonstrated in mouse GSTA4, the mitochondrial form is more heavily phosphorylated than the cytosolic form while possessing the same primary protein sequence (Robin et al., 2003). If post-translational modification is involved in the GSTZ1 translocation to mitochondria, modifications of residues around the GSH binding pocket may alter the conformation of this region in mitochondrial GSTZ1 and thus contribute to the reduced GSH affinity. Nevertheless, GSH is present at concentrations (2–10 mM) well above the  $K_m$  values in cytosol and mitochondria (Hansen et al., 2006); therefore, the difference in  $K_m$  for GSH should not affect or limit the rates of DCA dechlorination in either compartment under physiological conditions.

Inspection of the DCA metabolic pathway reveals that all but one of the enzymes involved in secondary biotransformation are located in the mitochondria (Supplemental Fig.1). Our study establishes a novel role of the mitochondrion in DCA primary biotransformation, which may allow efficient degradation of glyoxylate in mitochondria and therefore explain the fact that a large majority of DCA metabolites observed in vivo are derived from mitochondrial pathways of secondary biotransformation (Lin et al., 1993; James et al., 1998). However, generation of glyoxylate in the mitochondria may perturb the mitochondrial redox homeostasis because glyoxylate is an electrophile and may react with cellular macromolecules (Anderson et al., 2004). DCA-induced inactivation of GSTZ1 was observed in both cytosol and mitochondria of rats treated with 500 mg/kg/day DCA for 8 weeks. However, the question remains as to whether or not lower environmental and therapeutic doses of DCA would affect GSTZ1 similarly in the two compartments.

We unexpectedly observed a marked induction of cytosolic ALDH1A1 in the livers of DCA-treated rats, which we speculate to be caused by an increased level of oxidative stress in the livers because of DCA treatment. ALDH1A1 is a cytosolic and inducible isoform of the aldehyde dehydrogenase family that catalyzes the oxidation of medium-chain aliphatic aldehydes, including 4-hydroxynonenal and malondialdehyde (Alnouti and Klaassen, 2008). This is noteworthy because elevated levels of these indices of lipid peroxidation have been found in the sciatic nerves of rats treated with the same dose of DCA as used in the present study (Calcutt et al., 2009). Furthermore, increased production of reactive oxygen species and lipid peroxidation have been demonstrated in the livers of mice treated with high doses of DCA (Larson and Bull, 1992; Hassoun et al., 2010). Overexpression of ALDH1A1 has been shown to be an adaptive response to oxidative stress (Choudhary et al., 2005; Leonard et al., 2006). Therefore, we tentatively attribute the induced expression of cytosolic ALDH1A1 to be a secondary response to DCA exposure.

The GSTZ1 antibody-cross-reacting protein was shown to be a rat mitochondrial matrix protein but exhibited varying degrees of expression in the cytosol depending on the liver condition. Its appearance in the cytosol of frozen control liver could be the result of mitochondrial membrane lesions caused by freezing the liver and thawing it on ice (Pallotti and Lenaz, 2007). It is notable that the expression of this protein was further increased in the DCA-treated cytosol. We speculate that this altered expression is a combined result of freeze-thawing the liver and further leakage of mitochondrial protein caused by DCA treatment. DCA can induce oxidative stress (Larson and Bull, 1992; Hassoun et al., 2010), a condition detrimental to mitochondrial membrane integrity (Fulda et al., 2010).

In conclusion, we demonstrate that the mitochondrion, known to be the site of DCA's pharmacological action on PDK, is also a site of DCA biotransformation. The reaction is catalyzed by GSTZ1, an enzyme colocalized in the cytosol and the mitochondrial matrix. GSTZ1 of both compartments is inactivated by high doses of DCA and exhibits the same  $^{APP}K_m$  values for DCA, but different  $^{APP}K_m$  values for GSH. The discovery of this organelle as a second site of DCA biotransformation provides a new perspective on understanding DCA metabolism.

#### Acknowledgments

We thank members of the Proteomics Facility at the Interdisciplinary Center for Biotechnology Research (University of Florida) for conducting the LC-MS/MS and N-terminal sequencing analysis; Dr. Mike Katovich for providing fresh rat livers for submitochondrial studies; and Yuan Gu and Ann M. Nichols (University of Florida) and Veronica Lopez (University of California, San Diego) for technical assistance.

#### Authorship Contributions

*Participated in research design:* Li, James, Calcutt, and Stacpoole.  
*Conducted experiments:* Li, James, McKenzie, and Calcutt.  
*Performed data analysis:* Li, James, McKenzie, and Calcutt.  
*Wrote or contributed to the writing of the manuscript:* Li, James, Calcutt, Liu, and Stacpoole.  
*Other:* Liu provided human liver samples.

#### References

- Alnouti Y and Klaassen CD (2008) Tissue distribution, ontogeny, and regulation of aldehyde dehydrogenase (Aldh) enzymes mRNA by prototypical microsomal enzyme inducers in mice. *Toxicol Sci* **101**:51–64.
- Ammini CV, Fernandez-Canon J, Shroads AL, Cornett R, Cheung J, James MO, Henderson GN, Grompe M, and Stacpoole PW (2003) Pharmacologic or genetic ablation of maleylacetoacetate isomerase increases levels of toxic tyrosine catabolites in rodents. *Biochem Pharmacol* **66**:2029–2038.
- Anderson WB, Board PG, and Anders MW (2004) Glutathione transferase  $\zeta$ -catalyzed bioactivation of dichloroacetic acid: reaction of glyoxylate with amino acid nucleophiles. *Chem Res Toxicol* **17**:650–662.
- Archer SL, Gomberg-Maitland M, Maitland ML, Rich S, Garcia JG, and Weir EK (2008) Mitochondrial metabolism, redox signaling, and fusion: a mitochondrial ROS-HIF-1 $\alpha$ Kv1.5 O<sub>2</sub>-sensing pathway at the intersection of pulmonary hypertension and cancer. *Am J Physiol Heart Circ Physiol* **294**:H570–H578.
- Board PG, Taylor MC, Coggan M, Parker MW, Lantum HB, and Anders MW (2003) Clarification of the role of key active site residues of glutathione transferase  $\zeta$ /maleylacetoacetate isomerase by a new spectrophotometric technique. *Biochem J* **374**:731–737.
- Calcutt NA, Lopez VL, Bautista AD, Mizisin LM, Torres BR, Shroads AL, Mizisin AP, and Stacpoole PW (2009) Peripheral neuropathy in rats exposed to dichloroacetate. *J Neuropathol Exp Neurol* **68**:985–993.
- Choudhary S, Xiao T, Vergara LA, Srivastava S, Nees D, Piatigorsky J, and Ansari NH (2005) Role of aldehyde dehydrogenase isozymes in the defense of rat lens and human lens epithelial cells against oxidative stress. *Invest Ophthalmol Vis Sci* **46**:259–267.
- Cornett R, James MO, Henderson GN, Cheung J, Shroads AL, and Stacpoole PW (1999) Inhibition of glutathione S-transferase  $\zeta$  and tyrosine metabolism by dichloroacetate: a potential unifying mechanism for its altered biotransformation and toxicity. *Biochem Biophys Res Commun* **262**:752–756.

- Fleischer S, McIntyre JO, and Vidal JC (1979) Large-scale preparation of rat liver mitochondria in high yield. *Methods Enzymol* **55**:32–39.
- Forner F, Foster LJ, Campanaro S, Valle G, and Mann M (2006) Quantitative proteomic comparison of rat mitochondria from muscle, heart, and liver. *Mol Cell Proteomics* **5**:608–619.
- Fulda S, Galluzzi L, and Kroemer G (2010) Targeting mitochondria for cancer therapy. *Nat Rev Drug Discov* **9**:447–464.
- Gallagher EP, Gardner JL, and Barber DS (2006) Several glutathione S-transferase isozymes that protect against oxidative injury are expressed in human liver mitochondria. *Biochem Pharmacol* **71**:1619–1628.
- Goto S, Kawakatsu M, Izumi S, Urata Y, Kageyama K, Ihara Y, Koji T, and Kondo T (2009) Glutathione S-transferase  $\pi$  localizes in mitochondria and protects against oxidative stress. *Free Radic Biol Med* **46**:1392–1403.
- Guo X, Dixit V, Liu H, Shrods AL, Henderson GN, James MO, and Stacpoole PW (2006) Inhibition and recovery of rat hepatic glutathione S-transferase  $\zeta$  and alteration of tyrosine metabolism following dichloroacetate exposure and withdrawal. *Drug Metab Dispos* **34**:36–42.
- Hansen JM, Go YM, and Jones DP (2006) Nuclear and mitochondrial compartmentation of oxidative stress and redox signaling. *Annu Rev Pharmacol Toxicol* **46**:215–234.
- Hassoun EA, Cearfoss J, and Spildener J (2010) Dichloroacetate- and trichloroacetate-induced oxidative stress in the hepatic tissues of mice after long-term exposure. *J Appl Toxicol* **30**:450–456.
- James MO, Cornett R, Yan Z, Henderson GN, and Stacpoole PW (1997) Glutathione-dependent conversion to glyoxylate, a major pathway of dichloroacetate biotransformation in hepatic cytosol from humans and rats, is reduced in dichloroacetate-treated rats. *Drug Metab Dispos* **25**:1223–1227.
- James MO, Fouts JR, and Bend JR (1976) Hepatic and extrahepatic metabolism, *in vitro*, of an epoxide (8-<sup>14</sup>C-styrene oxide) in the rabbit. *Biochem Pharmacol* **25**:187–193.
- James MO, Yan Z, Cornett R, Jayanti VM, Henderson GN, Davydova N, Katovich MJ, Pollock B, and Stacpoole PW (1998) Pharmacokinetics and metabolism of [<sup>14</sup>C]dichloroacetate in male Sprague-Dawley rats. Identification of glycine conjugates, including hippurate, as urinary metabolites of dichloroacetate. *Drug Metab Dispos* **26**:1134–1143.
- Keller A, Nesvizhskii AI, Kolker E, and Aebersold R (2002) Empirical statistical model to estimate the accuracy of peptide identifications made by MS/MS and database search. *Anal Chem* **74**:5383–5392.
- Lantum HB, Baggs RB, Krenitsky DM, Board PG, and Anders MW (2002) Immunohistochemical localization and activity of glutathione transferase  $\zeta$  (GSTZ1-1) in rat tissues. *Drug Metab Dispos* **30**:616–625.
- Larson JL and Bull RJ (1992) Metabolism and lipoperoxidative activity of trichloroacetate and dichloroacetate in rats and mice. *Toxicol Appl Pharmacol* **115**:268–277.
- Leonard MO, Kieran NE, Howell K, Burne MJ, Varadarajan R, Dhakshinamoorthy S, Porter AG, O'Farrelly C, Rabb H, and Taylor CT (2006) Reoxygenation-specific activation of the antioxidant transcription factor Nrf2 mediates cytoprotective gene expression in ischemia-reperfusion injury. *FASEB J* **20**:2624–2626.
- Lin EL, Mattox JK, and Daniel FB (1993) Tissue distribution, excretion, and urinary metabolites of dichloroacetic acid in the male Fischer 344 rat. *J Toxicol Environ Health* **38**:19–32.
- Michelakis ED, Sutendra G, Dromparis P, Webster L, Haromy A, Niven E, Maguire C, Gammer TL, Mackey JR, Fulton D, et al. (2010) Metabolic modulation of glioblastoma with dichloroacetate. *Sci Transl Med* **2**:31ra34.
- Mootha VK, Bunkenborg J, Olsen JV, Hjerrild M, Wisniewski JR, Stahl E, Bolouri MS, Ray HN, Sihag S, Kamal M, et al. (2003) Integrated analysis of protein composition, tissue diversity, and gene regulation in mouse mitochondria. *Cell* **115**:629–640.
- Mughal FH (1992) Chlorination of drinking water and cancer: a review. *J Environ Pathol Toxicol Oncol* **11**:287–292.
- Nesvizhskii AI, Keller A, Kolker E, and Aebersold R (2003) A statistical model for identifying proteins by tandem mass spectrometry. *Anal Chem* **75**:4646–4658.
- Pallotti F and Lenaz G (2007) Isolation and subfractionation of mitochondria from animal cells and tissue culture lines. *Methods Cell Biol* **80**:3–44.
- Pfanner N and Geissler A (2001) Versatility of the mitochondrial protein import machinery. *Nat Rev Mol Cell Biol* **2**:339–349.
- Polekhina G, Board PG, Blackburn AC, and Parker MW (2001) Crystal structure of maleylacetoacetate isomerase/glutathione transferase  $\zeta$  reveals the molecular basis for its remarkable catalytic promiscuity. *Biochemistry* **40**:1567–1576.
- Raza H, Robin MA, Fang JK, and Avadhani NG (2002) Multiple isoforms of mitochondrial glutathione S-transferases and their differential induction under oxidative stress. *Biochem J* **366**:45–55.
- Ricci G, Turella P, De Maria F, Antonini G, Nardocci L, Board PG, Parker MW, Carbonelli MG, Federici G, and Caccuri AM (2004) Binding and kinetic mechanisms of the  $\zeta$  class glutathione transferase. *J Biol Chem* **279**:33336–33342.
- Robin MA, Prabu SK, Raza H, Anandatheerthavarada HK, and Avadhani NG (2003) Phosphorylation enhances mitochondrial targeting of GSTA4-4 through increased affinity for binding to cytoplasmic Hsp70. *J Biol Chem* **278**:18960–18970.
- Sheffield J, Taylor N, Fauquet C, and Chen S (2006) The cassava (*Manihot esculenta* Crantz) root proteome: protein identification and differential expression. *Proteomics* **6**:1588–1598.
- Shrods AL, Guo X, Dixit V, Liu HP, James MO, and Stacpoole PW (2008) Age-dependent kinetics and metabolism of dichloroacetate: possible relevance to toxicity. *J Pharmacol Exp Ther* **324**:1163–1171.
- Stacpoole PW, Henderson GN, Yan Z, Cornett R, and James MO (1998) Pharmacokinetics, metabolism, and toxicology of dichloroacetate. *Drug Metab Rev* **30**:499–539.
- Stacpoole PW, Kurtz TL, Han Z, and Langae T (2008) Role of dichloroacetate in the treatment of genetic mitochondrial diseases. *Adv Drug Deliv Rev* **60**:1478–1487.
- Tong Z, Board PG, and Anders MW (1998a) Glutathione transferase  $\zeta$ -catalyzed biotransformation of dichloroacetic acid and other  $\alpha$ -haloacids. *Chem Res Toxicol* **11**:1332–1338.
- Tong Z, Board PG, and Anders MW (1998b) Glutathione transferase  $\zeta$  catalyses the oxygenation of the carcinogen dichloroacetic acid to glyoxylic acid. *Biochem J* **331**:371–374.

---

**Address correspondence to:** Dr. Margaret O. James, Department of Medicinal Chemistry, Health Science Center P6-20, University of Florida, P.O. Box 100485, Gainesville, FL 32610-0485. E-mail: mojames@ufl.edu

---